

Structural States of the Nucleosome*

(Received for publication, October 10, 1995, and in revised form, December 6, 1995)

Gregory J. Czarnota‡ and F. P. Ottensmeyer

From the Ontario Cancer Institute and the Department of Medical Biophysics, University of Toronto,
Toronto, Ontario M5G 2M9, Canada

The nucleosome is the fundamental component of the eukaryotic chromosome, participating in the packaging of DNA and in the regulation of gene expression. Its numerous interactions imply a structural dynamism. Previous biophysical studies under limited sets of conditions have not been able to reconcile structural differences and transitions observed. We have determined a series of nucleosome conformations over a >10,000-fold range in salt concentration using a combination of biochemical methods, spectroscopic electron microscopy, and three-dimensional reconstruction techniques for randomly oriented single particles. This study indicates several ionic strength-dependent nucleosome conformations and also reconciles the differences between currently existing divergent models for the nucleosome. At low ionic environments, the particle appears highly elongated, becoming more compact and prolate ellipsoidal as ionic strength is increased to 10 mM NaCl. At 30 mM NaCl, the particle exhibits a spheroidal conformation. As ionic strength is increased to 150 mM NaCl, the nucleosome conformation changes and becomes oblate. Above 450 mM NaCl, the structure becomes highly elongated again. The result of this study is a unifying concept in which the three-dimensional structure of the nucleosome is inferred to be dynamic in response to ionic interactions and in accord with biochemical and genetic studies.

The nucleosome is a nucleoprotein complex composed of DNA wrapped about a core of histone proteins (1, 2). Its canonical role in the cell is the packaging of DNA, although a number of recent biochemical and genetic studies have shown that the nucleosome is also an active macromolecular complex involved in the facilitation, modulation, and repression of gene expression (3–6). Nucleosome structure has previously been investigated by a number of diverse biophysical techniques, including measurements of fluorescence properties, circular dichroism, and sedimentation coefficient (7–13), which infer changes in conformation with changes in pH, ionic environment, and post-translational modifications. Despite this, crystallographic studies of nucleosome particles (14–17) using x-ray and neutron diffraction have consistently resulted in only one structure, an oblate ellipsoid. Moreover, a high resolution structure for the nucleosome core protein octamer determined using x-ray crystallography, when wrapped with model DNA, is con-

sistent with such an oblate form (18, 19). In contrast, studies using electron microscopy (EM)¹ and three-dimensional reconstruction techniques have indicated a different form consistent with a prolate ellipsoid (20–23). The reproducibility of the divergent results has prompted us to investigate the reason for the major differences between the structures. We have found that the structure of the nucleosome changes dramatically with ionic environment, as determined by biochemical methods, conformational characterization (21–23), and three-dimensional reconstruction techniques based on the principle of angular reconstitution (24–29). Our structural characterization indicates several ionic strength-dependent conformations of the nucleosome. One of these corresponds to the three-dimensional EM structure previously determined (20), while another corresponds to the crystallographic form of this particle (14–19). The study ranges from 0.0001 M to 1.75 M in ion concentration and shows the first three-dimensional reconstructions of different conformational states of the nucleosome by a single consistent technique. In total, the results not only reconcile long-standing differences observed between electron microscopic investigations of nucleosome structure (20–22) and other biophysical studies (14–19), but also corroborate structural changes observed at extremes of ionic strength (12, 13, 30).

EXPERIMENTAL PROCEDURES

Purification of Nucleosomes and Electron Microscopy—Calf thymus nucleosomes were purified (21) and then prepared and chemically fixed under different ionic conditions to preserve the corresponding particle conformation. Optimal fixation of nucleosomes prepared in ionic environments selected to sample stable nucleosomal states, discussed below (2), utilized both formaldehyde and glutaraldehyde to assure protein-protein and protein-nucleic acid cross-linking (21). In total, nucleosome structure was examined over a >10,000-fold range of ionic strength. Sedimentation and electrophoretic analyses were carried out to determine that nucleosome conformation was unchanged before and after cross-linking (Ref. 12 and this study). Electron microscopy was performed as described before (21) using electron energy-loss spectroscopic imaging to provide images of nucleosomes with phosphorus-enhanced contrast (20, 31–33) and also using cryoimaging in a darkfield mode. Both electron energy-loss spectroscopic imaging and darkfield EM were selected as substitutes for brightfield microscopy, specifically to eliminate the need for heavy atom ionic stains as contrast agents (34), which would change ionic environments. Although air-drying of nucleosome particles has typically been used for analyses using electron energy-loss spectroscopy (31–33), a number of different preparative methods were used here in order to rule out specimen preparation artifacts. Fixed nucleosomes were dried from salt solutions by blotting, air-dried from water, dried from a variety of solvents with a lower surface tension than water, and critical point-dried (21) to minimize surface tension forces even further. Nucleosome preparation for imaging included confirmatory experiments using freeze-drying since investigations have indicated that protein conformation can be preserved upon lyophilization (reviewed in Ref. 35). All preparative conditions gave consistent results in terms of electron microscopy and principal component analyses for any single ionic nucleosome environment. For consistency, except where indicated, the results shown are from nucleosomes prepared

* This work was supported by the MRC Canada, NCIC, and OCTRF. The costs of publication of this article were defrayed in part by the payment of page charges. This article must therefore be hereby marked "advertisement" in accordance with 18 U.S.C. Section 1734 solely to indicate this fact.

‡ Recipient of a Steve Fonyo Fellowship from the NCIC. To whom correspondence should be addressed: Div. of Molecular and Structural Biology, Ontario Cancer Inst., 610 University Ave., Toronto, Ontario M5G 2M9, Canada. Tel.: 416-946-2000 (ext. 4929) Fax: 416-946-6529; E-mail: gczarnot@oci.utoronto.ca.

¹ The abbreviations used are: EM, electron microscopy; TEA, triethanolamine.

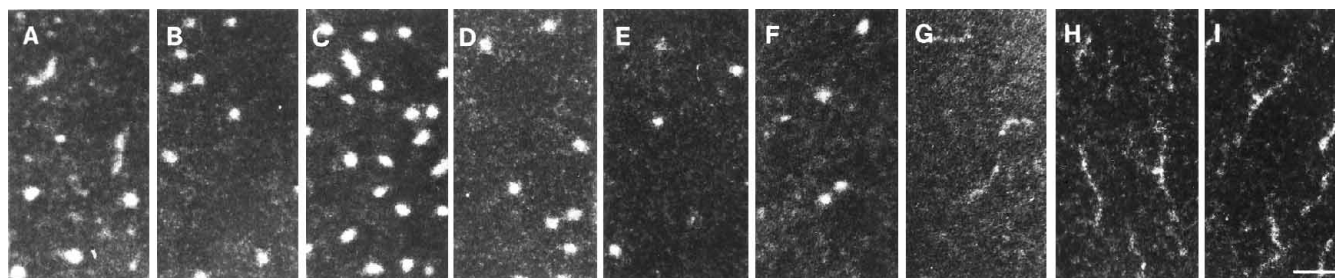


FIG. 1. **Images of highly purified calf thymus nucleosomes prepared in different ionic environments.** Shown are nucleosomes prepared in the presence of 0.1, 3.5, 10, 30, 150, 400, 750, 1200, and 1725 mM NaCl (A–J, respectively) and dried from amyl acetate to minimize surface tension forces. Nucleosomes in A and B were prepared in low concentration buffer (0.15 mM TEA-Cl, pH 7.4) to ensure a low effective ionic environment. In C–I, particles were prepared in more concentrated buffer (15 mM TEA-Cl and 2 mM EDTA, pH 7.4). In separate experiments, specimens in the presence of <30 mM NaCl were also prepared in the higher concentration buffer, which affected nucleosome conformation similar to equivalent monovalent salt concentrations. The scale bar indicates 200 Å.

under different ionic conditions and then fixed and dried from ethanol and amyl acetate to reduce disruptive surface tension forces.

Nucleosomes were prepared for conformational analysis in ionic environments of 0.1, 3.5, 10, 30, 150, 400, 750, 1200, and 1725 mM NaCl. These specific conditions were chosen as they correspond to points midway between ionic environments indicated by other studies as transition points in nucleosome structure: 0.4 mM NaCl (10), 1 mM NaCl (7, 8, 11), 6 mM NaCl (8, 11), 16 mM NaCl (11), 50 mM NaCl (11), 250 mM NaCl (9, 11), 550 mM NaCl (9, 12), 950 mM NaCl (10, 12, 13), and 1450 mM NaCl (12, 13). Particles in the presence of <30 mM NaCl were prepared in low concentration buffer (0.15 mM triethanolamine (TEA) chloride, pH 7.4) to ensure a low effective ionic environment. At all other ionic strengths, nucleosomes were prepared in more concentrated buffer (15 mM TEA-Cl and 2 mM EDTA, pH 7.4) for additional buffering (21). Specimens in the presence of <30 mM NaCl were also prepared in the higher concentration of buffer in order to investigate the effects of buffer on changes in nucleosome conformation. The effect of buffer was found to be similar to that of monovalent salt. Triethanolamine was chosen as a buffer in order to eliminate potential complications caused by buffers such as Tris-Cl since triethanolamine does not contain amino groups that would react with the glutaraldehyde fixative. Nucleosome particles in each ionic environment were at a concentration of 0.3 μ g/ml and were kept in this ionic environment for 24 h prior to fixation. Nucleosomes were then fixed in the selected ionic environments with the optimal conditions of 0.5% (w/v) glutaraldehyde and 3.0% (w/v) formaldehyde for 24 h at 4 °C as described before (21). The effects of divalent cations (MgCl_2 and MnCl_2) were also tested by including various concentrations of these salts in some of the preparations of nucleosomes.

Conformational Characterization of Nucleosomes from Their Micrographs—Nucleosome conformation was analyzed using principal component analysis. An explanation of this method was given by Zabal *et al.* (21) and is expanded below. Particles at all ionic strengths and buffer concentrations and prepared for electron microscopy as described above were analyzed in terms of dimensions and gross conformation. Statistical tests of significance, analyses of variance, and principal component analyses were carried out using the SAS statistical analysis system (21). Comparisons of various preparative methods (air-drying *versus* critical point drying *versus* drying from solvents) were made using nucleosome core particles prepared in 10 mM NaCl. A confirmatory comparison using freeze-dried nucleosome core particles was also carried out. A first principal component with an inclination near horizontal was used as a criterion for a prolate conformation; a near vertical direction indicated an oblate conformation. Inclinations near 45° indicated a spheroidal conformation. This is discussed further below. A mean length/width value of >4 was used as a criterion for a conformation being referred to as extended.

Three-dimensional Image Reconstruction of Nucleosomes—Three-dimensional reconstructions of nucleosomes were determined for nucleosome particles fixed with formaldehyde and glutaraldehyde in the presence of 10, 30, and 150 mM NaCl and the more concentrated buffer (15 mM TEA-Cl and 2 mM EDTA, pH 7.4). Specimens were prepared for electron microscopy using critical point drying to minimize surface tension forces during specimen drying (21). A comparison in this study using optimally chemically fixed nucleosome core particles indicated that freeze-drying results were equivalent to those obtained using critical point drying. Given these results and to be consistent with our previous investigations (20, 21), specimens were not prepared for imaging in vitreous ice. Additionally, most three-dimensional reconstructions

from single particles imaged in ice have resulted in resolutions worse than 30 Å, whereas previous reconstructions of critical point-dried fixed nucleosomes have indicated better resolutions (20).

Reconstructions were carried out using the quaternion-assisted approach of angular reconstitution (26, 27) for reconstructing non-crystalline randomly oriented biological macromolecules from their electron micrographs. The methods utilized have been used previously by us in the reconstruction of several biological macromolecules (26–28, 36, 37) and recently in modified form by Serysheva *et al.* (29). Our methods utilize sinograms and sinogram correlation functions (24, 25) and the central axis theorem (38) to determine the angular orientations of images of randomly oriented biological macromolecules with no internal symmetry. Sinograms and sinogram correlation functions were calculated as described before (26–28). The initial orientation angles of the reconstructions were refined iteratively by a quaternion vector approach as discussed by Farrow and Ottensmeyer (26). Resolution measurements were made as described by Czarnota *et al.* (28) using a phase residual approach with a conservative cutoff of 45°. Radii of gyration for reconstructions were calculated as described before (20).

RESULTS

Nucleosome Core Particles—Purification and analysis of purified nucleosomes prior to cross-linking in different ionic environments indicated that particles were composed of 146 ± 3 base pairs of DNA and stoichiometric quantities of histones H2A, H2B, H3, and H4. Analyses of cross-linking were carried out as described before (21) and indicated that fixation prevented nucleosome histone disassociation in the presence of various detergents and at high temperatures. Analyses of gel electrophoretic mobility and sedimentation coefficients using the particles prepared in 10 mM NaCl and the more concentrated buffer indicated virtually identical gel mobilities (R_F values of 0.59 and 0.60 prior to and after fixation, respectively) as well as sedimentation coefficients ($s_{20,w}$ values of 11.1 ± 0.9 and 11.2 ± 0.9 prior to and after fixation, respectively).

Electron Microscopy and Conformational Characterization of Nucleosomes—Images of highly purified calf thymus nucleosomes in different ionic environments are shown in Fig. 1. Significant gross differences between the different populations of nucleosomes are visible to the unaided eye (e.g. Fig. 1, E *versus* D), indicative of the existence of different conformational states. To analyze more subtle shape differences at near physiological monovalent cation concentration, a method of conformational characterization known as principal component analysis was used in correlation with analyses of particle length, width, and length/width distributions. This conformational characterization of nucleosome structure spanned the complete range of ionic strengths used; representative results are given in Fig. 2, and a compilation of primary results is presented in Fig. 3 and in Table I.

The representative results in Fig. 2 illustrate the differences between four different ionic strength populations of nucleosomes ranging from particles prepared in the presence of 10 mM

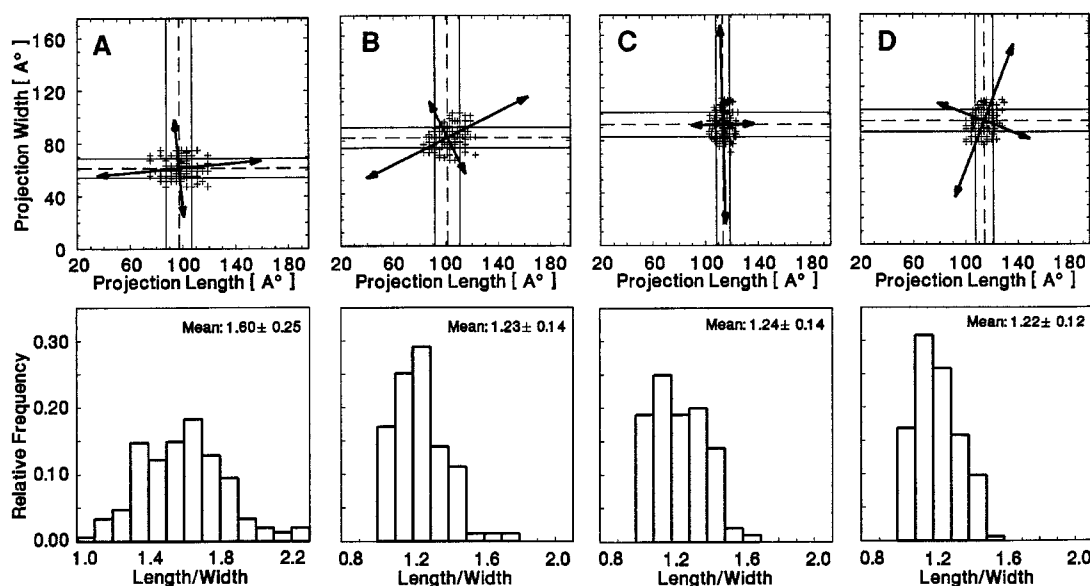


FIG. 2. **Conformational characterization of nucleosomes.** The panels give representative results of conformational determination by principal component analysis. A–D are results of a conformational analysis by principal component analysis for nucleosomes prepared in the presence of the higher ionic strength buffer and 10, 30, 150, and 400 mM NaCl, respectively. The lower panels show corresponding distributions of length/width values as histograms. The method of conformationally characterizing nucleosomes by principal component analysis is described in detail elsewhere (21). The longest arrow in each of the upper panels represents the best fit line through the scatter of paired length and width measurements as calculated by principal component analysis. The best fit line in A (upper panel) is consistent with a prolate ellipsoid, while the nearly vertical best fit line in C is consistent with an oblate ellipsoid. B is consistent with an intermediate form. Dimensional analysis of a perfect spheroid would generate a cluster of points resembling a half-circle about a point with equivalent length and width and a first principal component with an inclination of 45°. Tendencies toward greater or lesser slopes would indicate an oblate or prolate character, respectively. Scatters of points in each of the upper panels have been trimmed to exclude statistical extremes (21). Dashed lines indicate mean values, and solid lines indicate mean values ± 1 S.D. The differences between data in all these panels are statistically significant to a 95% confidence level (see “Results” for details). Mean ratios ± 1 S.D. in the lower panels are indicated by the numbers in the upper right corner of each histogram. The number of images analyzed is given in Table I (part A and B).

NaCl to particles prepared in the presence of 400 mM NaCl plus 15 mM TEA and 2 mM EDTA. The differences in the inclination of the first principal component among these different populations indicate differences in nucleosome conformation between these samples. The near horizontal first principal component in Fig. 2A, which corresponds to the best fit line determined by an analysis of variance, is in agreement with a prolate conformation (21). This conformation has mean projection length and mean projection width values consistent with those of previous studies (20–23). At 150 mM NaCl, this best fit line is nearly vertical, indicating an oblate conformation. The analysis at 30 mM NaCl indicates a best fit line that is consistent with an intermediate form between a prolate and an oblate form. Differences between the different ionic strength forms of the nucleosome are also reflected in the corresponding length/width distributions of images of single particles (Fig. 2, lower panels), although such representations do not readily permit direct structural inferences in terms of an ellipsoidal conformation.

Statistically Significant Differences between Ionic Strength-dependent Nucleosome Conformations—Statistical analysis of the results required care. As can be seen in Fig. 2 (lower panels), the mean projection length/width ratios for nucleosomes at 30, 150, and 400 mM NaCl are virtually identical even though the mean values of length, width, and their distributions are different (Table I, parts A and B; Fig. 2, upper panels). Analyses of paired length and width measurements (representative measurements in Fig. 2, A–D) indicated statistically significant differences between ionic strength-dependent nucleosome preparations. Since analyses were carried out between sets of paired length and width measurements, either a significant difference between the length measurements or a significant difference between the width measurements, or both, indicated that one set exhibited statistically significant differences with respect to another. Tests between mean lengths,

between mean widths, and between variances in length measurements or between variances in width measurements were carried out, also indicating statistically significant differences. For example, in a comparison between nucleosomes prepared in 10 and 30 mM NaCl, the F-test indicated statistically significant different distributions between length distributions (95% confidence level). The F-test also indicated statistically significant differences between the distributions of measured widths. The *t* test (95% confidence level, $t > 2.3$) indicated statistically significant differences between the mean lengths of nucleosomes prepared in 10 mM NaCl in comparison with nucleosomes prepared in 30 mM NaCl. Similarly, the *t* test indicated a statistically significant difference between the mean particle widths of the two preparations. Each preparation had statistically significantly different lengths and widths in comparison with the preparation in the closest higher ionic strength.

The differences between nucleosomes in 150 and 400 mM NaCl appeared by visual inspection to be less significant since each set had approximately equal mean projection lengths and approximately equal mean projection widths. Nevertheless, principal component analysis of the paired projection length and width measurements of each set indicates significant differences in variance, consistent with a change in shape from oblate to more spheroidal, at 150 and 400 mM NaCl, respectively (Fig. 2, C versus D; inclination of the first principal component changes from 90° to 68°, Table I, part B). The *t* test also indicates statistically significant differences in width measurements between these two ionic strength-dependent populations (95% confidence level). Significant differences between the variances of these sets of width measurements were indicated by the F-test to a 95% confidence level. In general, the appropriateness of the use of these tests was confirmed by the Shapiro-Wilk test, indicating that sets of measurements could be considered to have normal distributions. The results of

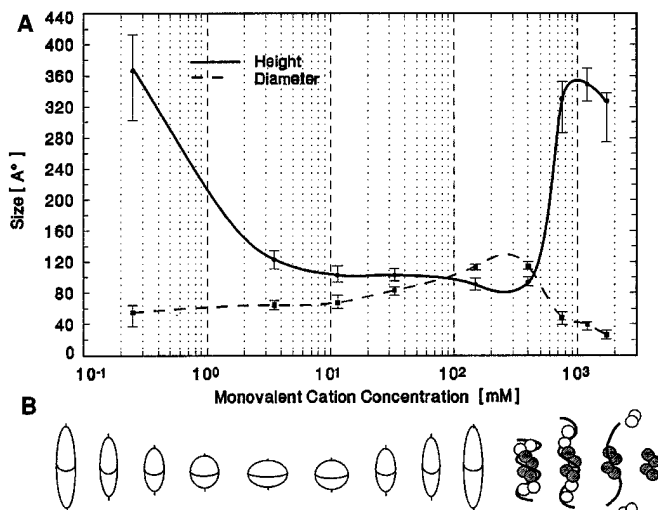


FIG. 3. A compilation of primary results of the characterization of ionic strength-dependent nucleosome conformations. A shows the median observed axial length and equatorial measurements for nucleosomes in a variety of ionic environments. The bars indicate first and third quartiles. At 150 mM NaCl, the minimum dimension observed was 60 Å. An additional set of measurements exists for the lowest ionic environment shown in this panel (see Table I, part A), but is not included on this figure for the sake of clarity. Dimensions of individually measured particles are given in Table I (part A and B), and details are described under "Results." Heights and diameters were from mean projection length and mean projection width values given in Table I (parts A and B). If the conformation was determined to be prolate, then the mean projection length was taken as the height and the mean projection width as the diameter. If the conformation was oblate, then the projection length was taken as the particle diameter, and the mean projection width was taken as the height (see Zabal *et al.* (21)). B indicates shapes and schematic representations of the various nucleosome structures deduced from electron microscopy and conformational characterization by principal component analysis. The schematic structure of the nucleosome (not to scale) is shown with increasing ionic strength from left to right. Spherical structures would correspond to the points of equal height and diameter. Dimensions given below 10 mM NaCl are for specimens in the presence of the less concentrated buffer (see "Experimental Procedures"). For detailed discussion of conformations, see "Results."

these tests were confirmed by the use of distribution-free non-parametric tests such as the Mann-Whitney test. This test also indicated statistically significant differences between the nucleosome populations at different ionic strengths. At the higher ionic environments (750 mM NaCl and above), where the Shapiro-Wilk test indicated that sets of measurements did not have normal distributions, the non-parametric analyses were used exclusively.

Different Nucleosome Conformations—Overall, the results indicate, with one exception (discussed below), that the nucleosome assumed a measurably different and constant conformation at each intertransitional ionic concentration tested. These nucleosome structures ranged from highly extended (length > 350 Å) at the low ionic strengths, through a prolate form at 10 mM NaCl consistent with the previous three-dimensional EM reconstruction (20), to an oblate shape at 150 mM NaCl approximating the crystallographic conformation (14–19). Above 400 mM NaCl, the nucleosome structure became prolate again and then elongated further. At 1200 and 1725 mM NaCl, the nucleosome became highly extended, and mass measurements were consistent with models in which the histones dissociate as H2A-H2B dimers at 900 mM NaCl and as (H3-H4)₂ tetramers at 1450 mM NaCl (12, 13). Using divalent cations (MgCl₂ or MnCl₂), we observed similar transitions at 35-fold lower concentrations (10), confirming earlier results (21–23). Monovalent TEA buffer was found to be equivalent in

effect to monovalent salt. The results were consistent regardless of the drying method: using optimally chemically fixed nucleosome core particles, critical point drying yielded equivalent results to freeze-drying; drying from amyl acetate was very similar to critical point drying; and air-drying, which does not minimize surface tension forces, resulted in particles that were larger in length and in width, as would be expected from distortion due to flattening of the structure (data not shown).

Only one distinct conformation for the nucleosome was generally detected in each ionic environment examined by an analysis of length and width measurements and by gel electrophoretic analyses (described below). One exception was 0.1 mM NaCl, at which two forms of the nucleosome were visualized with distinctly different images, inconsistent with a single conformation. One form was significantly more elongated and slender than the other (mean length/width ratio of 8 *versus* 1.2), suggesting that this selected ionic environment was in a transition zone between two nucleosome conformations. This interpretation is supported by other work (30) that indicated a similar major transition in this region of ionic strength (0.1–3 mM NaCl). Additionally, gel mobility experiments of particles prepared at 0.1 mM NaCl, described below, were consistent with two populations of particles. In contrast, a more compact population with the same relative mass was not visualized in electron micrographs at other ionic environments where elongated forms were visualized (*e.g.* 750 mM NaCl, *cf.* Figs. 1G and 3 and Table I, part B). Additionally, for particles prepared at this ionic environment (750 mM NaCl), gel mobility experiments indicated only one migrating form.

Electrophoresis had previously been used to indicate a similar mobility (and by inference, shape) between unfixed and fixed nucleosomes. To assess that the morphology of fixed nucleosomes seen by electron microscopy could be corroborated with that of the same nucleosomes in solution, electrophoresis of these particles in nondenaturing gels was carried out (Fig. 4). In agreement with biophysical theories (39, 40), slow migration of particles correlated with an elongated shape as determined via electron microscopy, and fast migration correlated with a compact shape. Consistent with this observation, the two forms of nucleosomes visualized at 0.1 mM NaCl were represented by two bands on the electrophoresis gel. At every other ionic concentration, only one band was identified in gel electrophoretic experiments, indicating by this criterion that both two-dimensional and three-dimensional analyses of nucleosome structure were carried out on a single homogeneous conformational form of the nucleosome core particle.

Three-dimensional Image Reconstruction of Nucleosomes—To provide direct three-dimensional evidence for a number of these conformations, low resolution three-dimensional structures of the nucleosome at three ionic strengths, 10, 30, and 150 mM NaCl, were determined using electron microscopy and image reconstruction techniques (26–28, 36). Calculated image orientations indicated relatively uniform distributions of image orientations used in each reconstruction. Only slight tendencies toward exhibiting preferred orientations were evident, as may be expected for specimens that have different shapes but are generally undistorted by preparative methods that minimize surface tension forces, such as the critical point drying used here.

The three-dimensional reconstructions are given in Fig. 5. At 10 mM NaCl, the structure of the nucleosome (Fig. 5A) was a prolate form that was consistent with the previous three-dimensional EM reconstruction. At 30 mM NaCl, the structure was virtually spherical with only a slight prolate tendency (Fig. 5B), while at 150 mM NaCl, the reconstructed nucleosome was distinctly oblate, approximating the shape and size of the crys-

TABLE I

Results of principal component analyses of nucleosomes prepared in the presence of different ionic strengths and the less concentrated (part A) and the more concentrated (part B) buffers

In part A, the less concentrated buffer contained 1.5 mM TEA-Cl, pH 7.4, and 2 mM EDTA. For more details, see "Experimental Procedures." Two populations were identified from image analysis of the particle at 0.1 mM NaCl. See "Results" for discussion. In part B, the more concentrated buffer contained 15 mM TEA-Cl, pH 7.4, and 2 mM EDTA. Analysis of the particles at 30 mM NaCl generated a first principal component with an inclination approaching but $<45^\circ$, consistent with a spheroidal conformation with a prolate tendency. In contrast, the analysis of particles in the presence of 400 mM NaCl generated a first principal component with an inclination near but $>45^\circ$, indicative of a spheroidal form with an oblate tendency. See "Discussion" for more details.

| Nucleosomal ionic environment | Mean projection length ± 1 S.D. (No. of measurements) | Mean projection width ± 1 S.D. | Percentage variance described by first principal component | Inclination of first principal component | Mean length/width ± 1 S.D. | Inferred gross conformation |
|--|---|-------------------------------------|--|--|--------------------------------|-----------------------------|
| \AA | | | | | | |
| A. Low ionic strength buffer | | | | | | |
| 0.1 mM NaCl (population 1) | 358 ± 63 (51) | 49 ± 15 | 95.4 | -6.6° | 8.10 ± 3.43 | Extended |
| 0.1 mM NaCl (population 2) | 133 ± 13 (107) | 86 ± 9 | 68.9 | 14.1° | 1.19 ± 0.19 | Prolate |
| 3.5 mM NaCl | 123 ± 17 (145) | 66 ± 8 | 81.7 | 1.2° | 1.90 ± 0.36 | Prolate |
| 10 mM NaCl | 97 ± 10 (152) | 67 ± 8 | 61 | 7.9° | 1.48 ± 0.24 | Prolate |
| B. Higher ionic strength buffer | | | | | | |
| 0.1 mM NaCl | 131 ± 15 (144) | 84 ± 12 | 65 | 19.4° | 1.59 ± 0.27 | Prolate |
| 3.5 mM NaCl | 121 ± 18 (141) | 74 ± 8 | 83.9 | 6.96° | 1.64 ± 0.30 | Prolate |
| 10 mM NaCl | 99 ± 14 (143) | 63 ± 10 | 67.0 | 7.9° | 1.60 ± 0.25 | Prolate |
| 30 mM NaCl | 101 ± 10 (141) | 82 ± 8 | 69.2 | 26.7° | 1.23 ± 0.14 | Spheroidal |
| 150 mM NaCl | 114 ± 5 (148) | 92 ± 9 (min = 60 \AA) | 75.8 | 91.4° | 1.24 ± 0.14 | Oblate |
| 400 mM NaCl | 114 ± 7 (145) | 94 ± 8 | 62.3 | 68.9° | 1.22 ± 0.12 | Spheroidal |
| 750 mM NaCl | 325 ± 40 (143) | 48 ± 11 | 93.6 | 4.3° | 7.17 ± 4.56 | Extended |
| 1200 mM NaCl | 351 ± 27 (144) | 39 ± 6 | 94.4 | 0.9° | 9.23 ± 1.60 | Extended |
| 1725 mM NaCl | 312 ± 44 | 26 ± 5 | 98.9 | 0.7° | 12.19 ± 2.88 | Extended |

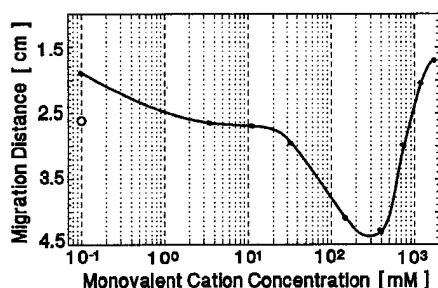


FIG. 4. **Electrophoretic analysis of nucleosomes from different ionic environments.** The migration distance of nucleosomes in a 5% polyacrylamide nondenaturing gel is shown in graph format for nucleosomes optimally fixed at the salt concentrations indicated with formaldehyde and glutaraldehyde to preserve nucleosome conformation prior to analysis (21). At 0.1 mM NaCl, a second band was present with a migration distance equivalent to that for nucleosomes in 3.5 mM NaCl (open circle; see "Results").

tallographic conformation (Fig. 5C). The values of axial height and equatorial diameter in conjunction with radii of gyration calculated from the three-dimensional reconstructions are given in Table II. The spatial resolution of 30 \AA in the three-dimensional reconstructions, determined using a phase residual approach (28) with a cutoff of 45° , a conservative measure of resolution, was isotropic since angular orientations used for each reconstruction were in general randomly distributed. However, the preparation at 10 mM NaCl did exhibit a slight

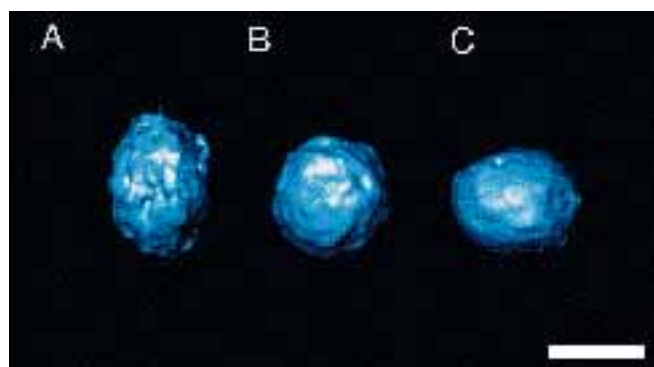


FIG. 5. **Three-dimensional structures for nucleosomes in three different ionic environments, determined by electron microscopy and image reconstruction techniques (26-28).** A-C are structures for the nucleosomes prepared in the presence of 10, 30, and 150 mM NaCl, respectively. These reconstructions have heights and diameters of 108 and 72 \AA , 99 and 80 \AA , and 80 and 110 \AA , respectively. All conformations are essentially circular when viewed from the top. Structures shown correspond to the theoretical volume for the combined nucleic acid and protein components of the nucleosome. The scale bar indicates 75 \AA .

tendency toward displaying side views, while the particles prepared in the presence of 150 mM NaCl tended to display views with a circular profile. To counteract these tendencies, image classification schemes (26, 27) were used to ensure that particular views of the particle were not under-represented.

TABLE II
 Characteristics of three-dimensional reconstructions including
 dimensions and calculated radii of gyration
 Comparisons with literature values are given under "Results."

| Nucleosomal ionic environment | Height | Diameter | Radius of gyration |
|-------------------------------------|--------|----------|-----------------------|
| | Å | Å | Å |
| 10 mM NaCl | 108 | 72 | 37.9 |
| 30 mM NaCl | 99 | 80 | 38.5 |
| 150 mM NaCl | 80 | 110 | 39.1 |

DISCUSSION

The compendium of our results indicates directly that the structure of the nucleosome has a propensity to change with ionic environment and shows the existence of numerous different ionic strength-dependent conformations that exhibit statistically significant differences. Our characterization of nucleosome structure by electrophoretic analyses, two-dimensional analyses of images, and three-dimensional electron microscopic structure determination ranges over >4 orders of magnitude of ionic environment and includes the direct determination of the three-dimensional structure of three different nucleosome conformations. The different ionic environments in this study were selected as points beyond and midway between ionic environments indicated in other studies as ionic strengths at which nucleosome structure changes: 0.4 mM NaCl (10), 1 mM NaCl (7, 8, 11), 6 mM NaCl (8, 11), 16 mM NaCl (11), 50 mM NaCl (11), 250 mM NaCl (9, 11), 550 mM NaCl (9, 12), 950 mM NaCl (11–13), and 1450 mM NaCl (12, 13). However, the corresponding structural changes in those studies were inferred or remained unaddressed.

The conformational changes detected in this study are consistent with other biophysical studies that have investigated nucleosome structure generally within narrow ranges of ionic environments (1, 2, 9) and may be similar in part to structural changes induced by physiologically important charge-modifying post-translational modifications (3, 4, 31–32, 41, 42). The potential of the nucleosome to undergo morphological changes is supported by early microscopic studies on polynucleosomes (43), although most of the non-canonical forms seen were referred to as unfolded (1, 43), and by other biophysical studies that have indicated that polynucleosomes undergo salt-dependent structural changes (44). Although comparisons with our work are suggestive, structural changes of polynucleosomes may not correspond directly to conformational changes of mononucleosome particles as investigated here since DNA length has also been found to affect transitions of the particle (8).

Our nucleosome structures agree with photo-footprinting results that indicate a highly elongated nucleosome structure below 0.3 mM NaCl; moreover, they support proposals of an elongated prolate nucleosome structure at this ionic environment (30). Above this ionic strength, at 3 mM NaCl, our results indicate that the nucleosome changes to a more prolate and less extended form. This is supported by hydrodynamic and fluorescence studies (7, 8, 10, 11) that indicate a major structural change as ionic strength is increased from 0.3 to 3 mM NaCl. At 10 mM NaCl, a prolate form for the nucleosome was observed in this study by conformational characterization and by three-dimensional reconstruction. Its shape and size are consistent with previous three-dimensional (20) and two-dimensional (21, 22, 23) analyses of images. A unique form for the nucleosome at 10 mM NaCl, distinct from that at lower salt concentrations, should exist since fluorescence and sedimentation studies indicate a change in structure between 3 and 10 mM NaCl (8, 11). The calculated radius of gyration (20) of 37.9 Å for this 10 mM

NaCl reconstruction (Table II) coincides with the experimental value of 37.6 Å determined by neutron scattering for nucleosomes in a similar ionic environment (45).

Another, more spherical form for the nucleosome is indicated by this study at 30 mM NaCl. This is supported by observations of a conformational change between 10 and 30 mM NaCl (11) and by neutron scattering experiments that indicate a spherical conformation in a virtually equivalent ionic environment (46). The radius of gyration for this reconstruction (Table II) was determined to be 38.5 Å, an increase from the value at 10 mM NaCl. The value determined using neutron scattering is larger as well, 39.4 Å (46).

Upon further increases in ionic strength to 150 mM NaCl, a major change in nucleosome structure occurs in which its shape becomes oblate. The existence of a modification in conformation upon increasing ionic strength from 30 to 150 mM NaCl is also supported by the work of others (11). The oblate form detected in this study at an ionic environment resembling physiological conditions (in terms of monovalent cation concentration) approaches the crystallographic nucleosome structure (14–17). The three-dimensional reconstruction exhibits the same 110-Å diameter as the crystallographic conformation (15) and also approximates the high resolution core histone octamer structure modeled with DNA (18, 19). However, each hemisphere of the nucleosome is 10 Å greater in height than that in the crystallographic conformation. This is not necessarily surprising given that the ionic conditions used are not the same as the crystallographic conditions that typically include divalent cations, polyamines, and detergents (14–19), resulting in a chemical environment with an overall higher effective ionic strength. In addition, it is possible that the exact edge-on view showing the minimum particle height was under-represented in the electron micrographs and therefore underweighted in the three-dimensional reconstruction. The calculated radius of gyration of 39.1 Å for this reconstruction (Table II) is close to calculated values that range from 39.2 to 40.9 Å for the particles that have conformations consistent with the canonical crystallographic structure (47–49).

A further conformational change to a less oblate form observed in this study by microscopy of particles prepared in the presence of 400 mM NaCl is supported by findings of a transition between 150 and 400 mM NaCl by fluorescence studies (9, 11). This change is consistent with the overall structural change of the nucleosome characterized by Dong *et al.* (50) in the range of 100–600 mM NaCl. Using detailed physicochemical analyses in that study, it was concluded that both DNA and histones exhibit changes as salt is increased in this range, consistent with a trend to a more relaxed secondary structure (50). At still higher ionic strengths, the nucleosome structure undergoes a major elongation and disruption as reflected in our micrographs of the particle and supported by a variety of studies (12, 13, 51). At 750 mM NaCl and higher ionic strengths, the particle appeared in our study as a highly extended bent rod. Above 950 mM NaCl, H2A-H2B dimer disassociation has been reported using circular dichroism and fluorescence spectroscopy (12, 13). This is consistent with our micrographs of the particle prepared in the presence of 1200 mM NaCl and evident as a thinning of the nucleosome particle (Figs. 1G and 3 and Table I, part B), a decrease in mass, as well as the appearance of smaller particles consistent with the relative mass of a H2A-H2B dimer (data not shown). At a still higher ionic strength, 1725 mM NaCl, the structure appears even thinner in micrographs (Figs. 1H and 3 and Table I, part B) and has a decreased mass, consistent with observations that (H3-H4)₂ tetramer dissociation occurs above 1450 mM NaCl (12, 13). However, as characterized by Yager and van Holde (52), the

observed nucleosome disassociation is expected to be more acute at the nucleosome concentration of $0.3 A_{260}/\text{ml}$ used here than at higher nucleosome concentrations.

In summary, the results presented here indicate that nucleosome structure changes with ionic environment, indicating the effects of pervasive ionic interactions and charge effects (18, 19, 53). This report provides a structural basis for the study of conformational changes elicited by divalent ions and by specific charge modifications as the result of physiological requirements during the cell cycle or differentiation such as the acetylation, phosphorylation, and poly(ADP-ribosyl)ation of nucleosomes, which result in altered structures (32, 33, 54, 55). It also explains directly the different structures obtained previously by three-dimensional reconstruction and by crystallography. Moreover, the results establish a consistency between changes in nucleosome conformation seen in structural studies and alterations of the nucleosome observed by genetic and biochemical approaches, which also indicate a dynamic nature for this biochemically active macromolecular complex.

REFERENCES

- Kornberg, R. D., and Klug, A. (1981) *Sci. Am.* **244**, 52–64
- van Holde, K. E. (1988) *Chromatin*, Springer-Verlag New York Inc., New York
- Turner, B. M. (1991) *J. Cell Sci.* **99**, 13–20
- Grunstein, M., Durrin, L. K., Mann, R. K., Fisher-Adams, G., and Johnson, L. M. (1992) in *Transcriptional Regulation* (McKnight, S. L., and Yamamoto, K. R., eds) pp. 1295–1315, Cold Spring Harbor Laboratory, Cold Spring Harbor, NY
- Lewin, B. (1994) *Cell* **79**, 397–406
- Wolffe, A. (1994) *Cell* **77**, 13–16
- Gordon, V. C., Knobler, C. M., Olins, D. E., and Schumaker, V. N. (1978) *Proc. Natl. Acad. Sci. U. S. A.* **75**, 660–663
- Burch, J. B., and Martinson, G. (1980) *Nucleic Acids Res.* **8**, 4969–4987
- Dieterich, A. E., and Cantor, C. R. (1981) *Biopolymers* **20**, 111–127
- Libertini, L. J., and Small, E. W. (1982) *Biochemistry* **21**, 3327–3334
- Chung, D., and Lewis, P. N. (1985) *Biochemistry* **24**, 8028–8036
- Oohara, I., and Wada, A. (1987) *J. Mol. Biol.* **196**, 399–411
- Oohara, I., and Wada, A. (1987) *J. Mol. Biol.* **196**, 387–397
- Bentley, G. A., Lewit-Bentley, A. L., Finch, J. T., Podjarny, A. D., and Roth, M. (1984) *J. Mol. Biol.* **176**, 55–75
- Richmond, T. J., Finch, J. T., Rushton, B., Rhodes, D., and Klug, A. (1984) *Nature* **311**, 532–537
- Uberbacher, E. C., and Bunick, G. J. (1989) *J. Biomol. Struct. & Dyn.* **7**, 1033–1055
- Struck, M. M., Klug, A., and Richmond, T. J. (1992) *J. Mol. Biol.* **224**, 253–264
- Arents, G., Burlingame, R. W., Wang, B. C., Love, W. E., and Moudrianakis, E. N. (1991) *Proc. Natl. Acad. Sci. U. S. A.* **88**, 10148–10152
- Arents, G., and Moudrianakis, E. N. (1993) *Proc. Natl. Acad. Sci. U. S. A.* **90**, 10489–10493
- Harauz, G., and Ottensmeyer, F. P. (1984) *Science* **226**, 936–940
- Zabal, M. M. Z., Czarnota, G. J., Bazett-Jones, D. P., and Ottensmeyer, F. P. (1993) *J. Microsc. (Oxf.)* **172**, 205–214
- Czarnota, G. J. (1993) *Proceedings of the 51st Annual Meeting of the Microscopy Society of America* (Bailey, G. W. and Reider, C. L., eds) pp. 194–195, San Francisco Press Inc., San Francisco, CA
- Czarnota, G. J., and Ottensmeyer, F. P. (1994) *Proceedings of the International Congress on Electron Microscopy* (Jouffrey, B., Colliex, C., Hernandez-Verdon, D., Schrever, J., and Thomas, D., eds) pp. 441–442, Les Éditions De Physique Les Ulis, France
- Goncharov, A. B., Vainshtein, B. K., Ryskin, A. I., and Vagin, A. A. (1987) *Sov. Phys. Crystallogr.* **32**, 504–509
- van Heel, M. (1987) *Ultramicroscopy* **21**, 111–124
- Farrow, N. A., and Ottensmeyer, F. P. (1992) *J. Opt. Soc. Am.* **9**, 1749–1760
- Farrow, N. A., and Ottensmeyer, F. P. (1993) *Ultramicroscopy* **52**, 141–156
- Czarnota, G. J., Andrews, D. W., Farrow, N. A., and Ottensmeyer, F. P. (1994) *J. Struct. Biol.* **133**, 35–46
- Serysheva, I. I., Orlova, E. V., Chiu, W., Sherman, M. B., Hamilton, S. L., and van Heel, M. (1995) *Nature Struct. Biol.* **2**, 18–23
- Brown, D. W., Libertini, L. J., Suquet, C., Small, E. W., and Smerdon, M. J. (1993) *Biochemistry* **32**, 10527–10531
- Locklear, L., Ridsdale, J. A., Bazett-Jones, D. P., and Davie, J. R. (1990) *Nucleic Acids Res.* **18**, 7015–7024
- Oliva, R., Bazett-Jones, D. P., Locklear, L., and Dixon, G. H. (1990) *Nucleic Acids Res.* **18**, 2739–2747
- Oliva, R., Bazett-Jones, D. P., Mezquita, C., and Dixon, G. H. (1987) *J. Biol. Chem.* **262**, 17016–17025
- Misell, D. L. (1977) in *Image Analysis, Enhancement and Interpretation* (Glauert, A. M. ed) pp. 199–244, Elsevier/North-Holland Publishing Co., New York
- Rupley, J. A., and Careri, G. (1991) *Adv. Protein Chem.* **41**, 37–172
- Ottensmeyer, F. P., and Farrow, N. A. (1992) *Proceedings of the 50th Annual Meeting of the Electron Microscopy Society of America* (Bailey, G. W., Bentley, J., and Small, J. A., eds) pp. 1058–1059, San Francisco Press Inc., San Francisco, CA
- Bazett-Jones, D. P., Mendez, E., Czarnota, G., Ottensmeyer, F. P., and Allfrey, V. G. (1996) *Nucleic Acids Res.*, in press
- Crowther, R. A., De Rosier, D. J., and Klug, A. (1970) *Proc. R. Soc. Lond. Ser. A* **317**, 319–340
- Svedberg, T., and Pederson, K. D. (1940) *The Ultracentrifuge*, Oxford University Press, London
- Scopes, R. K. (1988) in *Protein Purification: Principles and Practice* (Cantor, C. R., ed) pp. 199–235, Springer-Verlag New York Inc., New York
- Bertrand, E., Erard, M., Gómez-Lira, M., and Jürgen, B. (1984) *Arch. Biochem. Biophys.* **129**, 395–398
- Wu, R. S., Panusz, H. T., Hatch, C. L., and Bonner, W. M. (1984) *CRC Crit. Rev. Biochem.* **20**, 201–263
- Thoma, F., Koller, T., and Klug, A. (1979) *J. Cell Biol.* **83**, 403–427
- Hansen, J. C., Ausio, J., Stanik, V. H., and van Holde, K. E. (1989) *Biochemistry* **28**, 9129–9136
- Uberbacher, E. C., Ramakrishnan, V., Olins, D. E., and Bunick, G. J. (1983) *Biochemistry* **22**, 4916–4923
- Hjelm, R. P., Kneale, G. G., Suau, P., Baldwin, J. P., and Bradbury, E. M. (1977) *Cell* **10**, 139–151
- Glatzer, O. (1977) *J. Appl. Crystallogr.* **10**, 415–421
- Pardon, J. F., Worcester, D. L., Wooley, J. C., Cotter, R. I., Lilley, D. M. J., and Richards, B. W. (1977) *Nucleic Acids Res.* **4**, 3199–3214
- Suau, P., Kneale, G. G., Braddock, G. W., Baldwin, J. P., and Bradbury, E. M. (1977) *Nucleic Acids Res.* **4**, 3199–3214
- Dong, F., Nelson, C., and Ausio, J. (1990) *Biochemistry* **29**, 10710–10716
- Wilhelm, M. L., and Wilhelm, F. X. (1980) *Biochemistry* **19**, 4327–4331
- Yager, T. D., and van Holde, K. E. (1984) *J. Biol. Chem.* **259**, 4212–4222
- Moudrianakis, E. N., and Arents, G. (1993) *Cold Spring Harbor Symp. Quant. Biol.* **58**, 273–279
- Bode, J., Gomex-Lira, M. M., and Schröter, H. (1983) *Eur. J. Biochem.* **130**, 395–398
- Prior, C., Cantor, C. R., Johnson, E. M., Littau, V. C., and Allfrey, V. G. (1984) *Cell* **34**, 1033–1042